

## $B(E2)$ Values in $^{150}\text{Nd}$ and the Critical Point Symmetry X(5)

R. Krücken,<sup>1</sup> B. Albanna,<sup>1</sup> C. Bialik,<sup>1</sup> R. F. Casten,<sup>1</sup> J. R. Cooper,<sup>1</sup> A. Dewald,<sup>2</sup> N. V. Zamfir,<sup>1,3,4</sup> C. J. Barton,<sup>1,\*</sup>  
C. W. Beausang,<sup>1</sup> M. A. Caprio,<sup>1</sup> A. A. Hecht,<sup>1</sup> T. Klug,<sup>2</sup> J. R. Novak,<sup>1</sup> N. Pietralla,<sup>1,2</sup> and P. von Brentano<sup>2</sup>

<sup>1</sup>A. W. Wright Nuclear Structure Laboratory, Yale University, New Haven, Connecticut 06520

<sup>2</sup>Institut für Kernphysik, Universität zu Köln, 50937 Köln, Germany

<sup>3</sup>Clark University, Worcester, Massachusetts 01610

<sup>4</sup>National Institute for Physics and Nuclear Engineering, Bucharest-Magurele, Romania

(Received 11 December 2001; published 22 May 2002)

Lifetimes of states in  $^{150}\text{Nd}$  were measured using the recoil distance method following Coulomb excitation of  $^{150}\text{Nd}$  by a 132 MeV  $^{32}\text{S}$  beam. The experiment was performed at the Yale Tandem accelerator, employing the SPEEDY gamma-ray detector array and the New Yale Plunger Device. Reduced transition probabilities in  $^{150}\text{Nd}$  are compared to the predictions of the critical point symmetry X(5) of the phase/shape transition that occurs for the  $N = 90$  rare earth isotones. Very good agreement was observed between the parameter-free (apart from scale) X(5) predictions and the low-spin level scheme of  $^{150}\text{Nd}$ , revealing this as the best case thus far for the realization of the X(5) symmetry.

DOI: 10.1103/PhysRevLett.88.232501

PACS numbers: 21.60.Fw, 21.10.Re, 27.70.+q

Phase transitions play a very important role in many areas of physics, and it is of general interest to understand the critical point behavior of a system undergoing a phase transition. Recently, a major breakthrough was made in the understanding of the critical point behavior of nuclei undergoing a phase/shape transition from spherical to deformed shapes. In two Letters Iachello introduced new critical point symmetries [1,2] that allowed parameter-free—except for scale—predictions of the excitation energies and electric quadrupole ( $E2$ ) strengths of electromagnetic transitions for nuclei at the critical point of a phase/shape transition. The predictions result from solving a five-dimensional Hamiltonian that is based on the quadrupole shape parameters  $\beta$  and  $\gamma$  and the three Euler angles as the coordinates (Bohr-Hamiltonian) and the realization that, at the critical point of the phase transition, the potential in the  $\beta$  degree of freedom can be approximated by a simple square-well potential. The treatment of the  $\gamma$  degree of freedom differs depending on whether the transition goes from spherical to  $\gamma$ -unstable deformed or axially symmetric ( $\gamma = 0^\circ$ ) deformed nuclei. However, in both cases the  $\beta$  and  $\gamma$  degrees of freedom are decoupled. For the E(5) critical point symmetry [1] (spherical to deformed  $\gamma$  unstable) the potential is flat in the  $\gamma$  direction, while in the case of the X(5) critical point symmetry [2] (spherical to axially deformed) a harmonic oscillator potential is used in the  $\gamma$  direction. In both cases the solution of the square-well potential leads to analytical solutions for the energies that are zeros of Bessel functions of, in case of the X(5) symmetry, irrational order.

This new theoretical concept of critical point symmetry was backed up experimentally by finding empirical realizations of each case,  $^{134}\text{Ba}$  for the E(5) case [3] and  $^{152}\text{Sm}$  for the X(5) case [4]. However, it is crucially important to find further empirical cases in order to test if this new concept is of wide use or just a unique curiosity. In case of the X(5) symmetry, the  $N = 90$  isotones of  $^{152}\text{Sm}$  are

the natural place to further test this symmetry. As already pointed out in Ref. [4], the yrast energies of  $^{150}\text{Nd}$  are even closer to the X(5) predictions than those of  $^{152}\text{Sm}$ , making this nucleus particularly interesting.

It is therefore the purpose of this Letter to report on the measurement of level lifetimes and branching ratios in  $^{150}\text{Nd}$ , giving an accurate determination of 12 new reduced transition probabilities,  $B(E2)$ , and the revision of four others. Previous measurements of  $B(E2)$  values in  $^{150}\text{Nd}$  were determined via Coulomb excitation [5–9]. With the new data presented here, a comprehensive comparison is possible of energies and  $B(E2)$  values in  $^{150}\text{Nd}$  with those predicted by the X(5) symmetry. The agreement found reveals  $^{150}\text{Nd}$  as the second, and so far in fact the best, case of an empirical realization of the critical point symmetry X(5).

The lifetimes of excited states in  $^{150}\text{Nd}$  were measured by means of the recoil distance method (RDM). States in  $^{150}\text{Nd}$  were Coulomb excited by a 132 MeV  $^{32}\text{S}$  beam delivered by the ESTU Tandem accelerator of the A. W. Wright Nuclear Structure Laboratory (WNSL) at Yale University. The beam was incident on a 1 mg/cm<sup>2</sup> enriched  $^{150}\text{Nd}$  layer evaporated onto a 1.5 mg/cm<sup>2</sup> Ta foil used for mechanical support, which faced the incoming beam. The deexcitation  $\gamma$  rays were detected by the Ge detectors of the SPEEDY array [10] and recorded when coincident with backward scattered beam particles detected by an array of photodiodes covering an angular range from  $153^\circ$  to  $171^\circ$ . The forward recoiling nuclei had an average velocity of  $v = 0.025(1)c$  and were stopped in a 9.3 mg/cm<sup>2</sup> thick Nb stopper foil. Target and stopper foil were mounted inside the New Yale Plunger Device [11]. Data were collected for 20 distances between 5 and 800  $\mu\text{m}$  for 4 to 8 h each, with the longer runs performed at the shortest distances to be most sensitive to shorter lifetimes.

For each distance, spectra of  $\gamma$  rays detected at  $138.5^\circ$  and  $41.5^\circ$  were produced under the condition that the

energies of the coincident backscattered projectiles were in the energy range corresponding to scattering on  $^{150}\text{Nd}$ . This eliminated the  $\gamma$ -ray background from Ta Coulomb excitation.

Figure 1 shows  $\gamma$ -ray energy spectra measured at forward angles for distances of 5, 23, 65, and 200  $\mu\text{m}$ . One can clearly see the shifted and unshifted components of the 409, 469, and 546 keV transitions in  $^{150}\text{Nd}$ . The peak areas of both components were determined as a function of target-to-stopper distance. The ratio of the shifted (unshifted) peak area to the total area (sum of shifted and unshifted) was determined for each distance. The data were analyzed using the differential decay curve method (DDCM), which has been described in detail in Refs. [12,13]. Here we give only a very brief description of the analysis for a simple case.

If the level of interest is populated by transition  $B$  and depopulated by transition  $A$ , a value  $\tau$  for the lifetime can be calculated at each target-to-stopper distance  $x$  by

$$\tau(x) = \frac{F(x)}{G(x)} \equiv \frac{R_u^A(x) - \alpha R_u^B(x)}{v \cdot \frac{d}{dx} R_s^A(x)}, \quad (1)$$

where  $\alpha$  corrects for branching ratios and energy dependent detector efficiencies.  $R_{u,s}^{A,B}$  are the unshifted ( $u$ ) and shifted ( $s$ ) intensity ratios for transitions  $A$  and  $B$ , respectively, and  $v$  is the recoil velocity. Lifetime values  $\tau(x)$

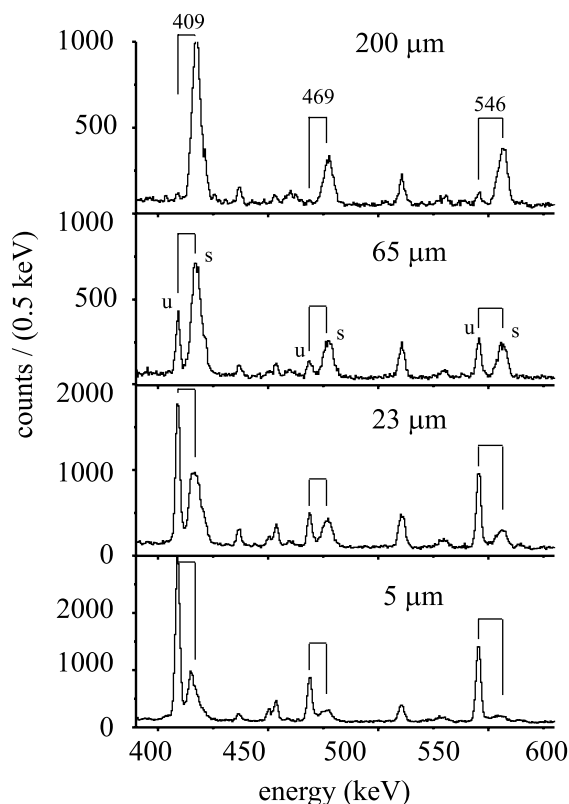


FIG. 1. Particle-energy gated gamma-ray spectra observed at  $41.5^\circ$  for distances of 5, 23, 65, and 200  $\mu\text{m}$ . Shifted ( $s$ ) and unshifted ( $u$ ) components of the 409 keV  $8_1^+ \rightarrow 6_1^+$  transition, the 469 keV doublet of the  $10_1^+ \rightarrow 8_1^+$  and  $2_2^+ \rightarrow 4_1^+$  transitions, and the 546 keV  $0_2^+ \rightarrow 2_1^+$  transition can be seen.

were extracted using Eq. (1) for each target-to-stopper distance  $x$  directly from the intensity ratios. Figure 2 shows  $\tau(x)$ ,  $F(x)$ , and  $G(x)$  for the 720 keV  $2_2^+ \rightarrow 2_1^+$  transition in  $^{150}\text{Nd}$  as a function of the distance  $x$ . The  $\tau$  values are constant within the range of distances where  $F(x)$  and  $G(x)$  are large, indicating the absence of significant systematic uncertainties in the analysis [12,13]. Table I summarizes the results of the RDM lifetime measurements and shows literature values for comparison. The agreement between the present results and the literature values [14] is generally very good. In most cases the uncertainties were significantly improved. Lifetimes were measured for the first time for the  $4_2^+$ ,  $4_3^+$ , and  $10_1^+$  levels. Significant deviations from earlier results were observed for the  $8_1^+$  and

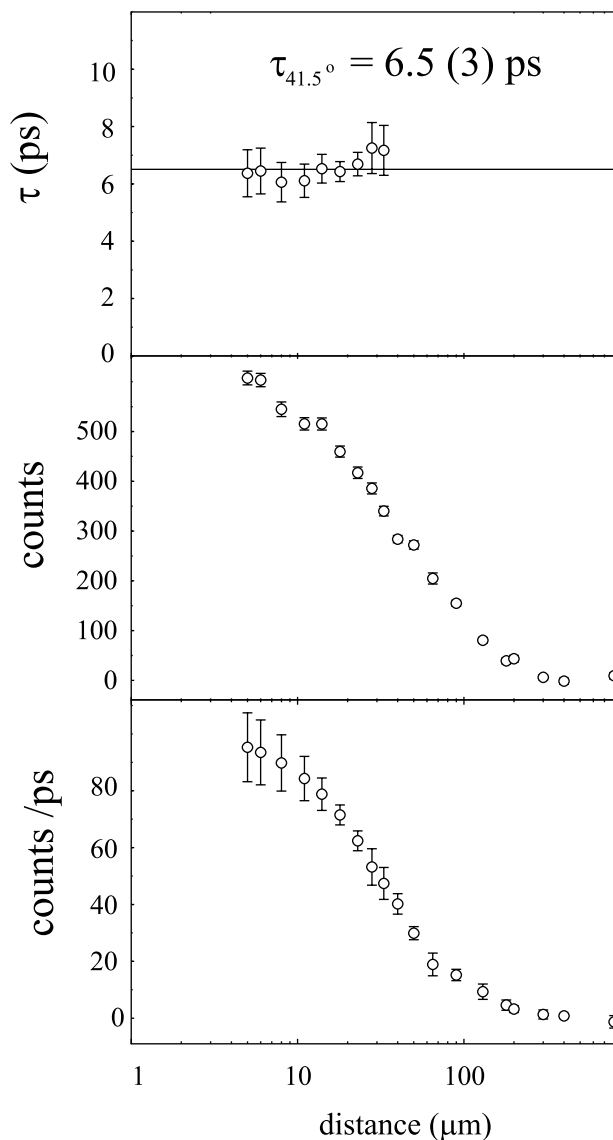


FIG. 2. Functions  $F(x)$  (middle),  $G(x)$  (bottom) of the DDCM analysis (see text for details) and the resulting lifetime values  $\tau(x)$  (top) at  $41.5^\circ$  for the 720 keV  $2_2^+ \rightarrow 2_1^+$  transition as a function of the target-to-stopper separation  $x$ . The weighted average of the lifetime values  $\tau(x)$ , deduced at this angle, is  $\tau(2_2^+) = 6.5(3)$  ps.

TABLE I. Level lifetimes  $\tau$  measured in the present experiment. For comparison lifetime values are shown, which were determined, unless indicated otherwise, from the adopted  $B(E2)$  values in Ref. [14].

$J^\pi$ ( $\hbar$ )	$E_x$ (keV)	$\tau$ (ps)	$\tau_{\text{prev.}}$ (ps)
$2_1^+$	130.2		2164 (22)
$4_1^+$	381.5	87.1 (7)	91 (1)
$0_2^+$	675.4	8.9 (4)	7.8 (3)
$6_1^+$	720.4	17.7 (1)	17.6 (10)
$2_2^+$	850.7	6.5 (2)	6.6 (10)
$2_3^+$	1062.0	2.1 (3)	2.12 (16)
$8_1^+$	1129.7	5.3 (5)	6.8 (4) <sup>a</sup> 5.8 (6) <sup>b</sup>
$4_2^+$	1137.8	4.8 (4)	
$4_3^+$	1350.2	2.9 (8)	
$10_1^+$	1598.7	3.7 (2)	

<sup>a</sup>Reference [15].

<sup>b</sup>Reference [7].

$0_2^+$  levels. In the case of the  $8^+$  values our new result agrees well with that of the previous RDM experiment [7] but not with the Coulomb excitation value stemming from the private communication by Fraser and Greenberg [15]. The literature value for the  $0_2^+$  level goes back to the same source [15]. Because of the good agreement of our results with the previous measurements for other states we trust in our new values for the lifetimes of these levels.

In addition to the measurement of lifetimes, the large statistics and high resolution of our data enabled us to precisely determine branching ratios for the decay of the populated levels. For the first time the branching ratios of the  $\gamma$  decay of the  $4_2^+$  and  $4_3^+$  levels were measured, while those for the  $2_2^+$  and  $2_3^+$  levels were revised.

Using the present values of the branching ratios and (except for the  $2_1^+$  level) level lifetimes  $B(E2)$  values were determined for the  $E2$  transitions originating from these levels using the relation  $\tau^{-1} = 1.225 \times 10^9 (1 + \alpha)^{-1} E_\gamma^5 B(E2)$  [16], where the lifetime  $\tau$  is given in seconds, the gamma-ray energy  $E_\gamma$  in MeV, and the  $B(E2)$  value in  $e^2 \text{fm}^4$ . The conversion coefficients  $\alpha$  were deduced using Ref. [17]. Since multipole mixing ratios were not determined in the present work we have assumed that all transitions have pure  $E2$  character. Since no  $E0$  strength has been measured for  $^{150}\text{Nd}$ , we assumed that the  $0_2^+ \rightarrow 2_1^+$  transition is the only transition depopulating the  $0_2^+$  state. Because of the three new lifetimes and the new or revised branching ratios a total of twelve  $B(E2)$  values were newly determined. The accuracy of another four  $B(E2)$  values has been significantly improved. The right of Fig. 3 shows a partial level scheme of  $^{150}\text{Nd}$ . The numbers on the transition arrows are the  $B(E2)$  values given in Weisskopf units (W.u.). The left of the same figure shows the  $s = 1$  and  $s = 2$  levels of the X(5) description. The energy scale was normalized to the energy of the  $2_1^+$  level.  $B(E2)$  values are shown in W.u., normalized to the experimental  $B(E2; 2_1^+ \rightarrow 0_1^+)$  value. The  $2_3^+$  and  $4_3^+$  levels are not included in the

framework of the current X(5) predictions. These two states are most likely part of the excitation in the  $\gamma$ -degree of freedom, for which there is no analytical prediction in the current X(5) predictions. Future refined calculations of this critical point symmetry [18] will take this degree of freedom into account as well as the coupling between the  $\beta$  and  $\gamma$  degrees of freedom.

The overall agreement between the experimental energies and  $B(E2)$  values with those predicted by the X(5) symmetry is truly remarkable in light of the fact that these predictions are fixed by the properties of X(5) and are not parametrized (except for scale). As already pointed out in Ref. [4] the energy spacing of the yrast ( $s = 1$ ) states is in nearly perfect agreement with X(5), in fact better than for  $^{152}\text{Sm}$ . Also the energy of the  $0_2^+$  state is almost exactly predicted. Note that the energy ratio  $E(0_2^+)/E(2_1^+)$  is fixed in X(5) and cannot be adjusted to fit the data. Taken together, these results establish the second empirical realization of a critical point nucleus for this phase transition from spherical to axially deformed nuclei. Of course, other models, microscopic [19], geometric [20–22], and algebraic [23,24] are also able to predict collective behavior in transitional regions and play a valuable role in obtaining detailed fits. However, such models are based on parametrized Hamiltonians and therefore serve a different purpose than fixed benchmark descriptions such as X(5). The fact that any nuclei match these paradigms as closely as  $^{150}\text{Nd}$  and  $^{152}\text{Sm}$  is remarkable.

As is the case of  $^{152}\text{Sm}$  the energy spacing in the  $s = 2$  levels is considerably smaller in  $^{150}\text{Nd}$  as compared to X(5). This feature is actually not peculiar to X(5) but also found in other models used in this region. The good overall agreement of the yrast  $B(E2)$  values for  $^{150}\text{Nd}$  is illustrated in Fig. 4 where the normalized  $B(E2)$  values for X(5) and  $^{150}\text{Nd}$  are shown as a function of spin. Apart from the  $10^+ \rightarrow 8^+$  transition, the values for  $^{150}\text{Nd}$

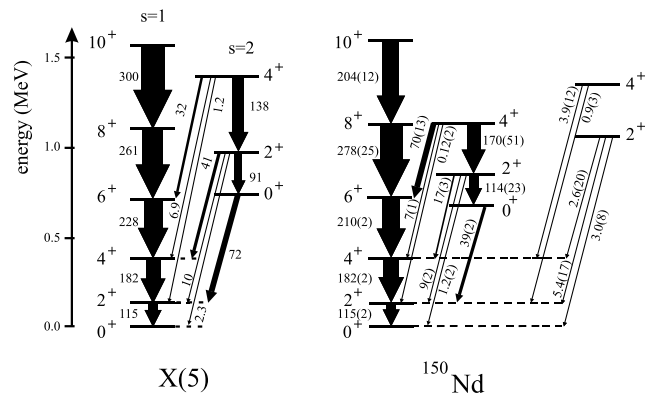


FIG. 3. Partial experimental level scheme of  $^{150}\text{Nd}$  (right) and the normalized predictions of the X(5) symmetry (left). The thickness of arrows indicates the  $B(E2)$  values, which are also given next to the arrows in Weisskopf units. The transition strengths for the X(5) predictions are normalized to the experimental best value of the  $2_1^+ \rightarrow 0_1^+$  transition. At the far right of the experimental level scheme, data on the  $2_3^+$  and  $4_3^+$  levels are shown for completeness.

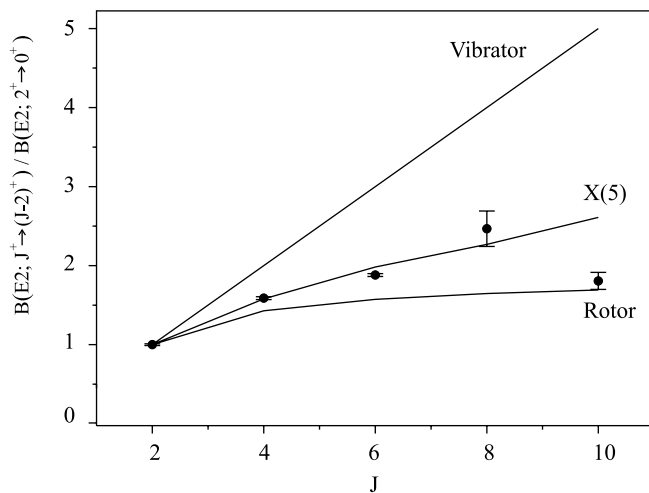


FIG. 4. Normalized  $B(E2)$  values for the yrast transitions in  $^{150}\text{Nd}$  in comparison to the predictions for the X(5) critical point symmetry, as well as for the geometric paradigms of harmonic vibrator and axially symmetric rotor.

are remarkably close to the X(5) predictions and show a significant deviation from the rotor values.

Regarding the crossover transitions from  $s = 2$  to  $s = 1$  states, we see for most transitions less than a factor of 2 difference between the experimental and predicted  $B(E2)$  values. Considering the simplicity of the calculations and the lack of free parameters of the model, this is a remarkable level of agreement. It is important to note that many observables change most rapidly in the vicinity of the critical point of the phase transition and therefore small deviations in structure from X(5) are amplified by these sensitive crossover  $B(E2)$  values. The fact that the average deviation of the crossover  $B(E2)$  values in  $^{150}\text{Nd}$  from X(5) is less than in  $^{152}\text{Sm}$  is consistent with the fact that the yrast energies and  $B(E2)$  values are also closer to X(5) in  $^{150}\text{Nd}$ . We also note here an interesting difference with  $^{152}\text{Sm}$  where there is an almost constant factor between the predictions and the data for these crossover  $B(E2)$  values, while in  $^{150}\text{Nd}$ , there are more fluctuations present. Additionally, for the 203 keV  $4_2^+ \rightarrow 1_1^-$  E1 transition, with a 13% gamma branching ratio, our lifetime data leads to a  $B(E1)$  value of 0.0011(3) W.u., which suggests some two-phonon octupole component in the wave function of the  $s = 2$  states [9]. This particular degree of freedom is not included in the X(5) picture.

In summary, we have measured lifetimes and branching ratios in  $^{150}\text{Nd}$  in a RDM experiment following Coulomb excitation of  $^{150}\text{Nd}$  with  $^{32}\text{S}$  projectiles. The new data allowed the precise determination of 12 new, and the revision of four other,  $B(E2)$  values. The low-spin structure of  $^{150}\text{Nd}$  was found to be the second, and so far the best, case of the empirical realization of the so-called X(5) critical

point symmetry of the phase transition between spherical and axially deformed nuclei.

We are grateful to F. Iachello for discussions of the new critical point symmetry. This work is supported by the U.S. DOE under Grants No. DE-FG02-91ER-40609 and No. DE-FG02-88ER-40417, as well as by the German Federal Minister for Education and Research (BMBF) under Contract No. 06OK958 and by the DFG under Contract No. Pi 393/1.

\*Present address: CLRC Daresbury, Warrington, U.K.

- [1] F. Iachello, Phys. Rev. Lett. **85**, 3580 (2000).
- [2] F. Iachello, Phys. Rev. Lett. **87**, 052502 (2001).
- [3] R. F. Casten and N. V. Zamfir, Phys. Rev. Lett. **85**, 3584 (2000).
- [4] R. F. Casten and N. V. Zamfir, Phys. Rev. Lett. **87**, 052503 (2001).
- [5] H. J. Wollersheim and Th. W. Elze, Z. Phys. A **280**, 277 (1977).
- [6] H. J. Wollersheim and Th. W. Elze, Nucl. Phys. **A278**, 87 (1977).
- [7] S. W. Yates, N. R. Johnson, L. L. Riedinger, and A. C. Kahler, Phys. Rev. C **17**, 634 (1978).
- [8] A. Ahmad *et al.*, Phys. Rev. C **37**, 1836 (1988).
- [9] P. A. Butler *et al.*, Acta Phys. Pol. B **24**, 117 (1993).
- [10] R. Krücken, in *Proceedings of the International Symposium on Advances in Nuclear Physics, Bucharest, Romania, 1999*, edited by D. Poenaru and S. Stoica (World Scientific, Singapore, 2000), p. 336.
- [11] R. Krücken, J. Res. Natl. Inst. Stand. Technol. **105**, 53 (2000).
- [12] A. Dewald and S. Harissopulos, and P. von Brentano, Z. Phys. A **334**, 163 (1989).
- [13] G. Böhm, A. Dewald, P. Petkov, and P. von Brentano, Nucl. Instrum. Methods Phys. Res., Sect. A **329**, 248 (1993).
- [14] E. derMateosian and J. K. Tuli, Nucl. Data Sheets **75**, 827 (1995).
- [15] I. Fraser and J. S. Greenberg (private communication); see C. M. Baglin, Nucl. Data Sect. B **18**, 223 (1976).
- [16] A. Bohr and B. Mottelson, *Nuclear Structure* (Benjamin, New York, 1969); (Benjamin, New York, 1975); (World Scientific, New York, 1998), Vol. I, p. 382.
- [17] R. S. Hager and E. C. Seltzer, Nucl. Data Sect. A, **4**, 1 (1968).
- [18] F. Iachello (private communication).
- [19] Krishna Kumar, Phys. Rev. Lett. **26**, 269 (1971).
- [20] A. S. Davydov and A. A. Chaban, Nucl. Phys. **20**, 499 (1960).
- [21] G. Gneuss, U. Mosel, and W. Greiner, Phys. Lett. **30B**, 397 (1969).
- [22] Jing-ye Zhang, M. A. Caprio, N. V. Zamfir, and R. F. Casten, Phys. Rev. C **60**, 061304 (1999).
- [23] A. Arima and F. Iachello, Phys. Rev. Lett. **35**, 1069 (1975).
- [24] O. Scholten, F. Iachello, and A. Arima, Ann. Phys. (N.Y.) **115**, 325 (1978).